

MATERIALS AND METHODS

Image Analysis

Lesion selection. Tumors and non-tumor anatomic features (vessels, organs, etc.) were considered PET-positive if they were visualized on PET with positive contrast relative to adjacent tissue. Radiolabel uptake was measured for tumors (a) that were identifiable on CT and (b) whose PET images were not obscured by overlap with the PET image of an adjacent PET-positive feature.

Uptake measurements, overview. PET image intensity or brightness was calibrated in units of radiolabel activity concentration based on scans of a large cylindrical phantom filled with a known, uniform concentration of ^{18}F . Radiolabel uptake in tissue was measured in terms of maximum voxel standardized uptake value (SUV_{max}), where “maximum voxel” refers to the voxel with maximum intensity within a given volume of interest (VOI). Once a VOI was defined, the software automatically indicated the location of the maximum voxel and calculated SUV_{max} .

Uptake measurements, ^{18}F -FDG. Analysis for a given tumor began with the ^{18}F -FDG scan. The ^{18}F -FDG tumor images were segmented via a maximum voxel-based thresholding (MVBT) technique (1). For a given lesion, a 3-dimensional rectangular VOI (threshold setting = 0% of maximum) was defined which contained the tumor image as identified by the study radiologist. The rectangular VOI was adjusted as needed to bring the maximum voxel within the tumor CT image. The PET images were inspected to determine whether the maximum voxel was overlapped by the PET-positive image of an adjacent feature. If not, SUV_{max} and the transaxial slice number for the maximum voxel were recorded. In practice, there were no instances in which a measurement of SUV_{max} (FDG) was rejected.

There were 2 tumors for which the rectangular VOI could not be adjusted to bring the maximum voxel within the tumor CT image while simultaneously encompassing the entire ^{18}F -FDG tumor image. For those lesions, the VOI was divided into 2 contiguous axial segments which together included the entire tumor PET image, and for which the maximum voxel for each segment lay within the tumor CT image. The largest value of $\text{SUV}_{\text{max}}(\text{FDG})$ for the combined segments was recorded.

Uptake measurements, ^{64}Cu -DOTA-trastuzumab. Patients underwent a PET/CT scan approximately 24 h after injection of ^{64}Cu -DOTA-trastuzumab (“Day 1” scan); all but 1 of the 18 patients had a second PET/CT scan approximately 48 h post injection (“Day 2” scan).

Alignment among the ^{18}F -FDG and ^{64}Cu -DOTA-trastuzumab PET/CT scans was optimized for each tumor. The CT scans were automatically coregistered via a rigid-body technique. The axial alignments of the ^{64}Cu PET/CT scans were then adjusted to maximize visual similarity of the tumor CT images with the tumor CT image for the ^{18}F scan. Corresponding slice numbers from the optimally-aligned scans were recorded to facilitate subsequent review.

The coregistered ^{64}Cu -DOTA-trastuzumab images were inspected in the region of the tumor CT image. If the maximum ^{64}Cu intensity in that region was clearly influenced by an adjacent feature, the tumor was recorded as non-measurable for uptake of ^{64}Cu -DOTA-trastuzumab.

For tumor ^{64}Cu -DOTA-trastuzumab images that were not rejected, the next step was to determine if the tumor image could be segmented by the same 3-D rectangular box, MVBT technique used for ^{18}F -FDG. If so, SUV_{max} [denoted $\text{SUV}_{\text{max}}(\text{tras})$] was determined

by a procedure analogous to that used for ^{18}F -FDG, including the requirement that the measurements not appear to be influenced by adjacent, PET-positive features. For the 2 tumors for which the FDG VOI comprised 2 axial segments, the trastuzumab VOIs were constructed as 2 contiguous axial segments matching those of the coregistered FDG VOI. There were also 1 other trastuzumab Day 1 tumor image and 2 other trastuzumab Day 2 tumor images for which 2 axial segments were required in order to bring the maximum voxel within the tumor CT image. In addition, there was 1 trastuzumab Day 2 tumor image that required 3 axial segments. In total, the 3-D rectangular box, MVBT technique was used to evaluate $\text{SUV}_{\text{max}}(\text{tras})$ for 78 of 87 Day 1 tumor images and 61 of 64 Day 2 tumor images.

Some ^{64}Cu -DOTA-trastuzumab tumor images (9 Day 1 and 3 Day 2) could not be segmented by the 3-D rectangular box, MVBT technique because of low tumor uptake relative to adjacent features. In those cases, the MVBT technique was used to define a VOI for the tumor ^{18}F -FDG image that approximately matched the boundary of the tumor CT image. The VOI for the tumor ^{64}Cu -DOTA-trastuzumab image was then drawn slice-by-slice on transaxial images to match the corresponding FDG isocontours with respect to size, shape and relationship to the tumor CT image, and $\text{SUV}_{\text{max}}(\text{tras})$ was evaluated for that VOI. One patient had two intra-hepatic tumors that were visualized with ^{18}F -FDG but whose ^{64}Cu -DOTA-trastuzumab images appeared equally intense with adjacent liver. For those, $\text{SUV}_{\text{max}}(\text{tras})$ was equated with the mean SUV for ^{64}Cu -DOTA-trastuzumab within the FDG-matched VOI.

Uptake measurements, special case. Random, count-dependent noise can be excessive near the ends of the axial range of a PET scan. Because of that, our SUV

measurements excluded the final 2 slices at either end of a scan. In no instance did the ^{18}F -FDG image of an evaluated tumor extend into the final 2 slices. For ^{64}Cu -DOTA-trastuzumab, however, the lesion extended into or beyond the final 2 slices for 7 of the 151 tumor images evaluated. In those cases, the SUV measurements employed VOIs for ^{64}Cu -DOTA-trastuzumab and ^{18}F -FDG that excluded the portion of the tumor that extended into or beyond the 2 end slices of the ^{64}Cu scan.

Tumor volume. As noted in the main text, tumor size was estimated from ^{18}F -FDG tumor images. For most tumors (89 of 98 evaluated), the CT boundary was well approximated by the isocontour for a PET threshold setting = 50% of maximum. There were, however, instances in which relatively low tumor-to-background contrast required the threshold be as high as 80% in order to bring the isocontour within the tumor CT image.

DISCUSSION

Comparison with Clinical Investigations Using ^{89}Zr -trastuzumab in Metastatic Breast Cancer

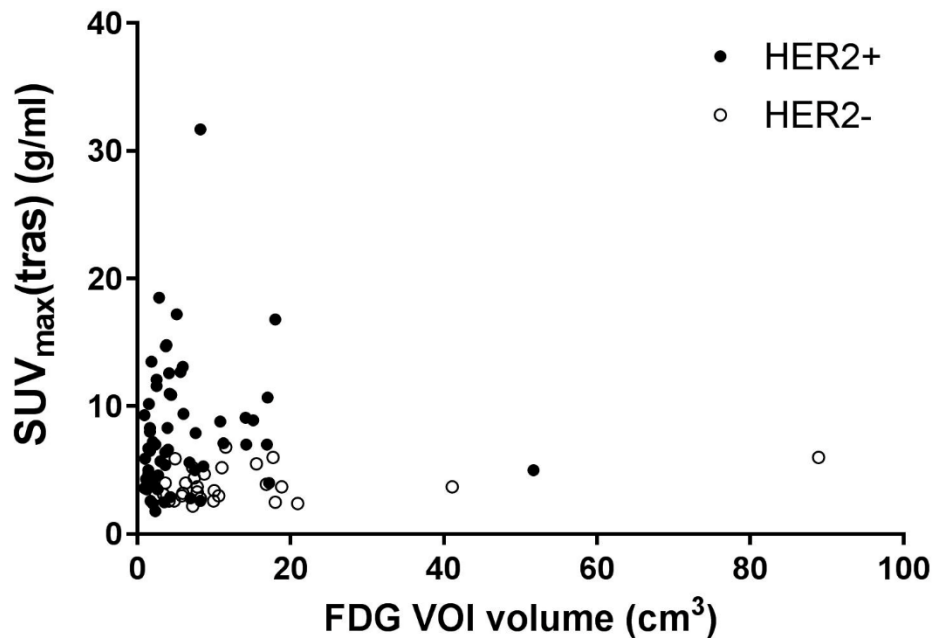
Gebhart, et al., (2) qualitatively categorized patients according to the proportion of FDG-avid tumor load showing ^{89}Zr -trastuzumab uptake > blood pool activity at 4 d post injection. Their findings (29% negative, 25% positive, 46% heterogeneous) are similar to our observations with ^{64}Cu -DOTA-trastuzumab in HER2+ patients. On Day 2 (main text Fig. 1C), 3 HER2+ patients had average SUV_{max} ($\langle \text{SUV}_{\text{max}} \rangle_{\text{pt}}$) that overlaps the $\langle \text{SUV}_{\text{max}} \rangle_{\text{pt}}$ distribution for HER2- patients (27% negative), 2 HER2+ patients had all SUV_{max} values for individual tumors > any SUV_{max} from a HER2- patient (18% positive),

and 6 HER2+ patients had SUV_{max} distributions that partially overlap the HER2- SUV_{max} distribution (55% heterogeneous).

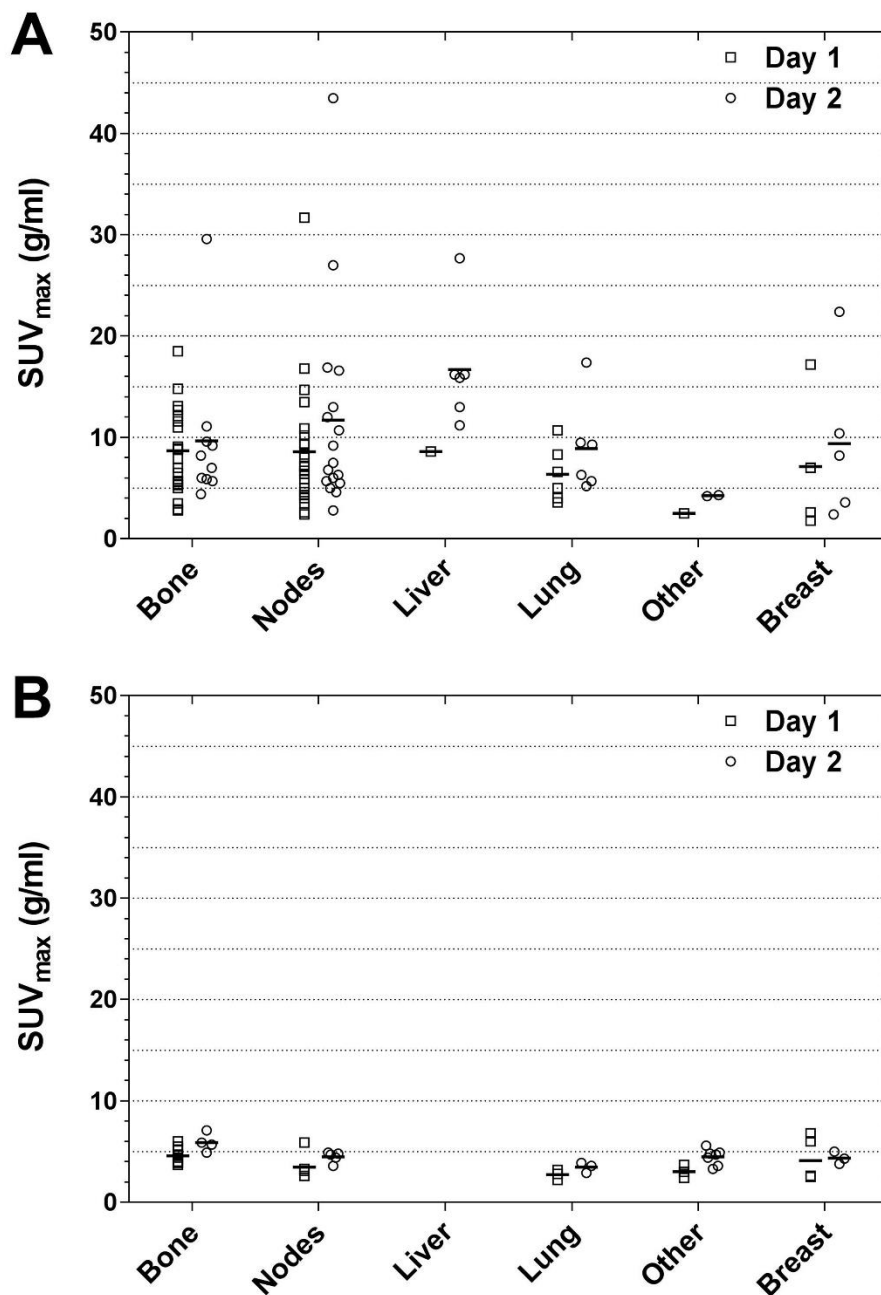
Ulaner, et al., (3) investigated tumor uptake of ^{89}Zr -trastuzumab in 9 patients with HER2- primary tumors. Five of the patients had a “suspicious focus” of uptake on ^{89}Zr -trastuzumab PET/CT performed 5 or 6 d post injection. Measured SUV_{max} in those lesions ranged from 4.6 to 9.7 g/mL; only the 2 with the lowest values (4.6 and 5.9 g/mL) were HER2+ on subsequent histopathology. These observations are consistent with ours (main text Fig. 1) both with regard to (i) the overlap of SUV_{max} distributions for nominally HER2+ and – disease and (ii) the absolute magnitude of SUV_{max} , given the difference in time between injection and scan for the 2 studies.

REFERENCES

1. Boellaard R, Krak NC, Hoekstra OS, Lammertsma AA. Effects of noise, image resolution, and ROI definition on the accuracy of standard uptake values: a simulation study. *J Nucl Med* 2004;45:1519-1527.
2. Gebhart G, Lamberts LE, Wimana Z, et al. Molecular imaging as a tool to investigate heterogeneity of advanced HER2-positive breast cancer and to predict patient outcome under trastuzumab emtansine (T-DM1): the ZEPHIR trial. *Annals of Oncology* 2016;27:619-624.
3. Ulaner GA, Hyman DM, Ross, DS, et al. Detection of HER2-positive metastases in patients with HER2-negative primary breast cancer using ^{89}Zr -Trastuzumab PET/CT. *J Nucl Med* 2016;57:1523-1528.



SUPPLEMENTAL FIGURE 1. Uptake of ^{64}Cu -DOTA-trastuzumab (Day 1) vs. metabolic tumor size. The figure shows Day 1 $\text{SUV}_{\text{max}}(\text{tras})$ plotted against tumor size, measured in terms of ^{18}F -FDG VOI volume. While the ranges of tumor size were similar for HER2+ and – patients, smaller tumors were proportionally more prevalent for the HER2+ than the HER2- group [volume (mean \pm SE)= $6.2 \pm 1.0 \text{ cm}^3$ (n = 57) vs. $13.1 \pm 3.1 \text{ cm}^3$ (n = 29); $P < 0.001$] (Wilcoxon rank sum test). However, neither group showed significant dependence of $\text{SUV}_{\text{max}}(\text{tras})$ on tumor size. Similar observations pertain to Day 2 $\text{SUV}_{\text{max}}(\text{tras})$.



SUPPLEMENTAL FIGURE 2. Uptake of ⁶⁴Cu-DOTA-trastuzumab vs. lesion site. Shown are the SUV_{max} data from (A) the HER2+ group (11 patients; number of lesions = 58 and 46 on Days 1 and 2, respectively) and (B) the HER2- group (7 patients; number of lesions = 29 and 28 on Days 1 and 2, respectively). Intra-patient means are represented by short horizontal lines. “Other” sites comprised pulmonary effusion for HER2+ patients and body

wall outside the breast for HER2- patients. There were no statistically significant differences among lesion sites for either HER2+ or HER2- patients on either day (F-test).